JOURNAL OF SOLID STATE CHEMISTRY **131,** 310–316 (1997)
ARTICLE NO. SC977386

$W_5As_{2.5}P_{1.5}$: The First One-Dimensional Vertex-Linked W_6 Cluster

F. Charki,*,† S. Députier,*,[1] P. Bénard-Rocherullé,* R. Guérin,* and E. H. El Ghadraoui‡

*Laboratoire de Chimie du Solide et Inorganique Moléculaire, UMR 6511, Avenue du Général Leclerc, 35042 Rennes Cédex, France; †Faculté des Sciences Dhar El Mehrez, Université Sidi-Mohamed Ben Abdallah, Fès, Morocco; and ‡Faculté des Sciences et techniques, Université Sidi-Mohamed Ben Abdallah, Fès, Saïss, Morocco

Received September 30, 1996; in revised form March 5, 1997; accepted March 11, 1997

A new ternary phase $W_5As_{2.5}P_{1.5}$ has been synthesized and investigated by means of X-ray powder diffraction. The tetragonal unit cell dimensions are $a = 9.4729$ (3) Å and $c = 3.2414$ (2) Å (space group $I4/m$ with $Z = 2$). The crystal structure has been refined by the Rietveld method using the structure Mo_5As_4 (Ti_5Te_4-type) as a related model ($R_F = 0.030$ and $R_P = 0.116$ for 160 reflections and 30 refined parameters). In the structure, the metalloid sublattice (As, P) is wholly disordered and there is no interaction between the metalloid atoms, while W–W bonding leads to the formation of octahedral W_6 clusters inserted in X_8 cubes (X = As, P). The significant aspect of this structure consists of the condensation of these W_6X_8 units through two opposite tungsten atoms. This results in the formation of one-dimensional columns with the composition $W_4W_{2/2}X_{8/2}$ (W_5X_4) parallel to the c-axis of the unit cell. Such a condensation of octahedral W_6 clusters has never been observed in solid state chemistry, the only examples of octahedral W_6 clusters being found in halide and chalcogenide chemistry but as isolated units. A general survey on Ti_5Te_4 or derivative-type structure compounds is also given. © 1997 Academic Press

INTRODUCTION

The binary systems Mo–As and W–As were studied many years ago (1, 2). Now it is well known that four phases occur in the Mo–As system: $MoAs_2$ of $NbAs_2$-type (3), Mo_2As_3 (4), Mo_5As_4 of Ti_5Te_4-type (5), and "MoAs" of MnP-type. The last compound does not exist as a binary since its stabilization needs either the substitution of at least 5 at.% Mo by a 3*d* element (Ti, V, Cr, Mn, Fe, Co), e.g., $Fe_{0.05}Mo_{0.95}As$, or the substitution of about 10 at.% As by phosphorus i.e., $MoAs_{0.9}P_{0.1}$ (6, 7). In the case of the W–As system, the only observed binaries are WAs_2 and W_2As_3, which are isostructural to the corresponding Mo-containing phases (2, 4). But astonishingly, neither W_5As_4 nor WAs have been found and our attempts to stabilize the binary "WAs" by substitution of either a 3*d* element for W or P for As were unsuccessful since the obtained compounds were $Fe_{0.8}W_{0.2}As$ and $WAs_{0.1}P_{0.9}$ which are the upper limits of the solid solutions $Fe_{1-x}W_xAs$ ($0 \le x \le 0.2$) and $WP_{1-x}As_x$ ($0 \le x \le 0.1$) of MnP-type structure (8). However, recently, during similar attempts to stabilize the binary "W_5As_4," a new ternary phase could be isolated which was found to be isostructural with the binary Mo_5As_4 of Ti_5Te_4-type. The present paper deals with the synthesis and the structure refinement of this new compound $W_5As_{2.5}P_{1.5}$, in which vertex-linked octahedral W_6 clusters have been evidenced. Secondly, a general survey of compounds having the Ti_5Te_4 or derivative structure is given, as well as the tungsten-containing compounds which also present octahedral but isolated W_6X_8 clusters (X = Cl, Br). Last, the metallic behavior of this new compound is also considered.

[1]To whom correspondence should be addressed.

EXPERIMENTAL DETAILS

Synthesis

The samples were prepared by direct combination of the elements: the starting materials were elementary arsenic (β-form), red phosphorus, and tungsten as powders, all with minimum purity >99.99%. The elements were intimately mixed and pressed into pellets in a glove box under purified argon to prevent oxidation, and then placed in quartz tubes which were evacuated to 10^{-3} Torr, sealed, and placed in a vertical furnace. Samples were first annealed at 1000°C for 3 days and after cooling, ground to powder, cold-pressed, sealed again, and then reannealed at 1000°C for 10 days to ensure homogeneity. The ternary phase $W_5As_{2.5}P_{1.5}$ has never been obtained pure; in all the cases, whatever the synthesis conditions and the different starting compositions, elemental tungsten was present as impurity. Attempts to obtain single crystals of the phase at higher temperature after slow cooling or by using I_2 as transport agent were unsuccessful.

X-Ray Powder Diffraction

For phase identification, routine X-ray powder diffraction patterns were recorded by means of a INEL (CPS 120)

0022-4596/97 $25.00
Copyright © 1997 by Academic Press
All rights of reproduction in any form reserved.

curved position-sensitive detector (PSD) which allows for a simultaneous data recording of a diffraction pattern over a range of 120° in 2θ. Elemental silicon was taken to determine a cubic spline calibration function to describe the 2θ vs channel number function.

For structure analysis, the X-ray powder diffraction data were collected with a Siemens D-500 high-resolution diffractometer using the Bragg–Brentano geometry. Pure monochromatic Cu$K\alpha_1$ radiation ($\lambda = 1.540598$ Å) was produced with an incident-beam curved-crystal germanium monochromator with asymmetric focusing. The alignment of the diffractometer was checked using the 00l reflections of fluorophlogopite mica standard material (NIST SRM 675) (9) and the zero-point error was estimated less than 0.005° (2θ). The instrument resolution curve exhibits a shallow minimum at about 40° (2θ) with a FWHM value of 0.065° (2θ). Additional details about the characteristics of this diffractometer have been reported elsewhere (10). The powder specimen was deposited in the sample holder using a top-loading procedure and data were scanned in steps of 0.02° (2θ) over the angular range 11–140° (2θ); a fixed counting time (26 s) was employed. The precise determination of peak positions was carried out by means of the Socabim fitting program PROFILE available in the software package DIFFRAC-AT supplied by Siemens.

POWDER DIFFRACTION PATTERN ANALYSIS

Indexing

As mentioned above, whatever the chemical route used for the preparation of the ternary phase $W_5As_{2.5}P_{1.5}$, elemental tungsten as impurity was always present. Consequently, the powder diffraction data sets studied in this work mirror the mixture of the two products.

An examination of the standard patterns suggested that all the diffraction lines, except those which belong to the impurity phase, could be indexed with a tetragonal unit cell with the parameters $a = 9.497$ (1) Å and $c = 3.249$ (1) Å by comparison with that of the binary Mo_5As_4 (5). This solution was confirmed by an indexing of more precise powder diffraction data: the peak positions of the 20 first lines (omitting those of W) were used, with an absolute error of 0.03° (2θ), for indexing the pattern of $W_5As_{2.5}P_{1.5}$ with the program DICVOL 91 (11). A unique tetragonal solution was found with the figures of merit $M_{20} = 79$ and $F_{20} = 60$ (0.0077, 43). This was consistent with the solution proposed in the first analysis.

After reviewing the complete available data by means of the computer program NBS*AIDS83(12), the refined cell dimensions were $a = 9.4729(3)$ Å, $c = 3.2414(2)$ Å, and $V = 290.87(2)$ Å^3 ($M_{20} = 127$ and $F_{30} = 91$ (0.0092, 36)). The powder diffraction data have been deposited with the ICDD (13). This unit cell was used to interrogate the NIST-CDF database (14), from which the chemically related material Mo_5As_4 with close cell parameters $a = 9.6005$ (6) Å, $c = 3.2781$ (4) Å, and $V = 302.14$ (5) Å^3 and known structure solved from single crystal data was found (5).

From a comparison between the two unit cells of the binary and ternary phases, a significant decrease in the volume from Mo_5As_4 to $W_5As_{2.5}P_{1.5}$ occurs, mainly due to a modification of the a parameter, the c dimension remaining roughly constant after the double substitution. This is not surprising since 30% of the As atoms were substituted by the P atoms and, in addition, the covalent radius of P ($r_P = 1.10$ Å) is smaller than that of As ($r_{As} = 1.18$ Å) (15). On the other hand, the total substitution of the Mo atoms by those of W should not induce any important change within the unit cell dimensions since the two corresponding metallic radii given in literature are nearly the same ($r_W = 1.38$ Å; $r_{Mo} = 1.37$ Å) (16). For example, nearly equal monoclinic unit cell parameters are found for the isostructural arsenides $MoAs_2$ ($a = 9.071$ Å, $b = 3.299$ Å, $c = 7.719$ Å, $\beta = 119.37$, $V = 201.3$ Å^3) and WAs_2 ($a = 9.085$ Å, $b = 3.318$ Å, $c = 7.690$ Å, $\beta = 119.52$, $V = 201.7$ Å^3) (1, 2).

The structure refinement of $W_5As_{2.5}P_{1.5}$ was undertaken from X-ray powder diffraction data assuming the centrosymmetric space group $I4/m$. During the Rietveld refinement procedure, it was found that it was better to take into account the contribution of the W impurity, whose line intensity was not negligible, than to exclude the corresponding angular regions. Finally, the two phases were refined together.

Structure Refinement of $W_5As_{2.5}P_{1.5}$

The structure of Mo_5As_4 (5) was selected as a starting model for the structure refinement of $W_5As_{2.5}P_{1.5}$. The least-squares refinement was performed with the Rietveld method using the program FULLPROF (17) based on the DBW3.2S (8804) (18). The final profile analysis refinement was carried out in the angular range 17–138° (2θ) and involved the following parameters for the two phases $W_5As_{2.5}P_{1.5}$ and W: 11 structural parameters including two scale factors, four atomic coordinates, and four isotropic temperature factors and among the 19 profile parameters two mixing parameters to define a θ-dependent pseudo-Voigt profile shape, six half-width parameters (U, V, W) to describe the angular dependence of the peak FWHM using the usual quadratic form in $\tan\theta$, one zero-point, one asymmetry parameter, three unit cell dimensions, and six coefficients in a polynomial function describing the background.

The details of the refinement are listed in Table 1. Figure 1 displays the final Rietveld refinement showing the best agreement between observed and calculated diffraction patterns. This fit corresponds to satisfactory profile factors ($R_P = 0.116$, $R_{WP} = 0.160$) and crystal structure model indicators for $W_5As_{2.5}P_{1.5}$ ($R_F = 0.030$, $R_B = 0.045$). The final

TABLE 1
Rietveld Full-Profile Refinement for $W_5As_{2.5}P_{1.5}$ and W

	$W_5As_{2.5}P_{1.5}$	W
Space group	$I4/m$	$Im3m$
Z	2	2
No. of atoms	3	1
Angular range (°2θ)	17–138	
Wavelength (Å)	1.540598	
Step scan increment (°2θ)	0.02	
No. of reflections	160	7
No. of structural parameters	9	2
No. of profile parameters	19	
R_F	0.030	0.019
R_B	0.045	0.029
R_P	0.116	
R_{WP}	0.160	

Note. The R factors are defined in (19).

TABLE 2
Positional and Isotropic Thermal Parameters with Their Standard Deviations for $W_5As_{2.5}P_{1.5}$

Atom	Position	x	y	z	B(Å^2)
W_I	2a	0	0	0	0.25(6)
W_{II}	8h	0.2964(2)	0.3782(2)	0	0.33(3)
(As, P)[a]	8h	0.0541(5)	0.2875(7)	0	0.8(2)

[a] Occupancy factors, $\tau_{As} = 0.62(1)$; $\tau_P = 0.38(1)$.

atomic parameters are given in Table 2 and selected bond distances in Table 3.

It must be noted that the refinement of the occupancy factors for As and P atoms in the same crystallographic position (0.0541, 0.2875, 0) led to a ratio $\tau_{As}/\tau_P = 1.63$ which is in very good accordance with the chemical formula $W_5As_{2.5}P_{1.5}$.

DISCUSSION

The structure of $W_5As_{2.5}P_{1.5}$ shows two kinds of W atoms which occupy the 2a (W_I) and 8h (W_{II}) positions of the space group $I4/m$ and only one kind of metalloid atom (As and P) in the 8h position. Thus, the metalloid sublattice

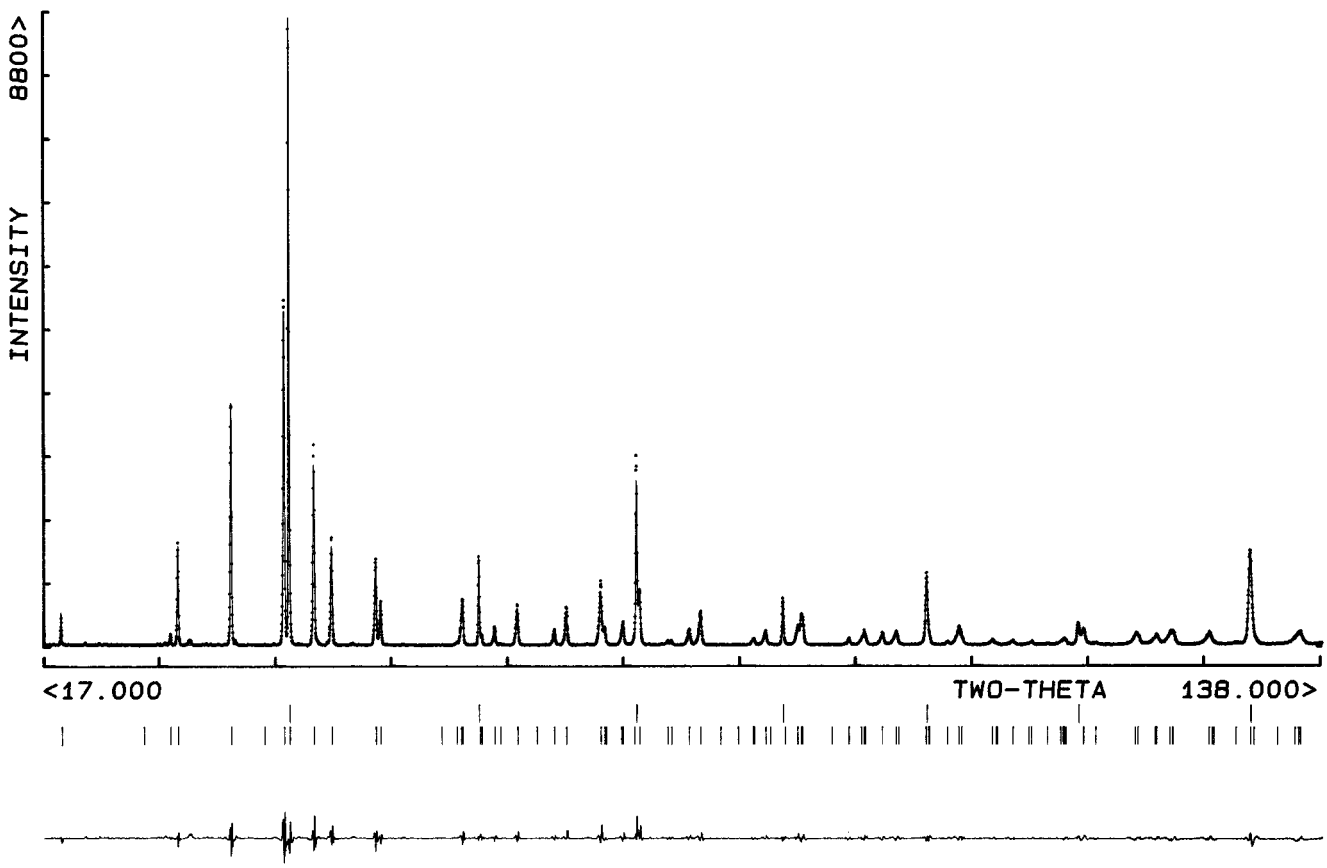

FIG. 1. Final Rietveld plot of the ternary phase $W_5As_{2.5}P_{1.5}$ and the elemental W. The upper trace shows the observed data as dots, while the calculated pattern is shown by a solid line. The lower trace is a plot of the difference observed minus calculated. The vertical markers show positions calculated for Bragg reflections: the upper marks correspond to W and the lower to the ternary compound.

TABLE 3
Selected Bond Distances (Å), Shorter than 3.45 Å, with Their Standard Deviations for $W_5As_{2.5}P_{1.5}$

W_I–4X^a	2.771 (7)	X–1 W_{II}	2.451 (5)
–8W_{II}	2.771 (4)	–2 W_{II}	2.457 (4)
–2W_I	3.241	–2 W_{II}	2.664 (5)
		–1 W_I	2.771 (7)
W_{II}–1X	2.451 (5)	–2 X	3.241
–2X	2.457 (5)	–4 X	3.355 (8)
–2X	2.664 (5)		
–2W_I	2.771 (4)		
–2W_{II}	3.049 (2)		
–2W_{II}	3.178 (3)		
–2W_{II}	3.241		

[a] X represents the metalloid atom (As, P).

is completely disordered (occupancy of about 60% of arsenic and 40% of phosphorus). There is no X–X bonding (X = As, P) since the smallest distance (3.241 Å), which corresponds to the c-axis, is considerably larger than the covalent diameter of arsenic (2.40 Å). It can be noticed that the nonmetal atom is surrounded by six metal neighbours (Fig. 2a), Table 3.

The W_I and W_{II} tungsten atoms exhibit two kinds of metalloid coordination which are square planar and pyramidal, respectively. As can be seen in Table 3, the W atoms are linked together by strong W_I–W_{II} bondings of 2.771 Å which is consistent with the shortest W–W distance of 2.74 Å in body-centered tungsten metal. These bondings involve the formation of octahedral W_6 clusters which are not regular since the intracluster W_{II}–W_{II} distance is 3.178 Å. These W_6 clusters are inserted in X_8 cubes of metalloid atoms giving rise to W_6X_8 units. The condensation of these units via opposite W atoms leads to a one-dimensional column with the composition $W_4W_{2/2}X_{8/2} = W_5X_4$ which develops along the c-axis of the unit cell (Fig. 2b). The W_5X_4 structure consists entirely of these columns arranged parallel to each other. It can be noticed that the chains of clusters are ordered in such a way, one relative to the other, that the interchain W_{II}–W_{II} distances are 3.049 Å, showing a significant compression of the W_6 octahedra along the c-axis (eight edges are 2.771 Å long while four edges in the (a, c) plane are 3.178 Å).

This is the first time that such a condensation of octahedral W_6 clusters has been observed in solid state chemistry. The only other examples of octahedral W_6 clusters are obtained in halide chemistry but these clusters are isolated, as occurs in the compounds CdW_6Br_{14} and $Cu_2W_6Br_{14}$ (cubic structure, space group $Pn3$) where the W–W distances are 2.632 Å (20, 21). Other molecular compounds with isolated W_6 clusters are known in solution chemistry as $[(n\text{-}C_4H_9)_4N]_2W_6Cl_{14}$ (2.607 Å) (22), $W_6S_8L_6$ (L = py, PEt_3) (23–25).

The $W_5As_{2.5}P_{1.5}$ structure is of the Ti_5Te_4 type which includes numerous binaries, such as V_5X_4 (X = S, Se, and

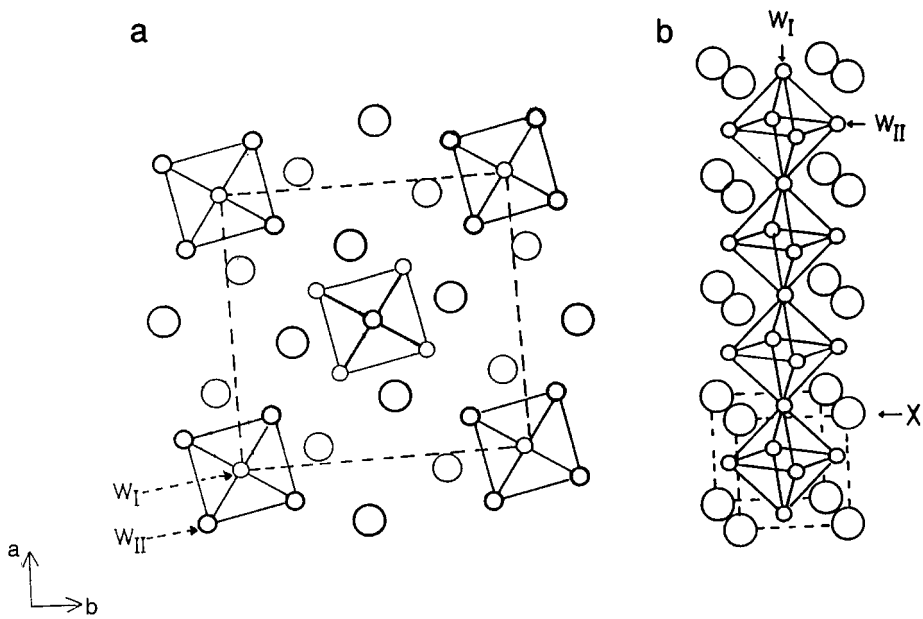

FIG. 2. Crystal structure of $W_5As_{2.5}P_{1.5}$. (a) Projection on the (001) plane. Large circles, metalloid atom (As, P); small circles, tungsten; fine and heavy circles are translated from each other by half a period of the projection direction. Octahedral W_6 clusters are emphasized. (b) One-dimensional chain of octahedral W_6 clusters inserted in X_8 cubes.

Sb), Nb_5X_4 (X = Se, Te, Sb), Ta_5Sb_4 (26–31), and Mo_5As_4, as previously mentioned. The main feature of the Ti_5Te_4-type structure is the existence of the infinite columns of M_6X_8 units (M = transition metal, X = nonmetal) arranged parallel to the c-axis (32). This disposition involves the occurrence of metalloid voids, formed by the X atoms between neighbouring chains of M_6 clusters, running along the c-axis. By filling these octahedral voids, interesting related Ti_5Te_4-type structures are built.

For example, Fig. 3 shows the projection of the structure of V_3As_2 which is a filled Ti_5Te_4 type (33). In this structure, additional vanadium atoms occupy the octahedral metalloid sites previously empty.

Intermediate steps of filling of these octahedral sites have been mentioned in the literature, especially in the case of Mo_5As_4 with elements such as copper, gallium, and aluminium (34); our own attempts to synthesize such ternary phases by inserting Cu, Fe, Cr, and Ga at 1050°C, by direct synthesis in evacuated and sealed silica ampoules, were not really successful. In addition to the presence of molybdenum as impurity, the results did not show significant variations of the unit cell parameters compared to those of Mo_5As_4. This means there is a very limited insertion of extra atoms in the binary at this temperature, as has been checked by microanalysis, for example, on the compound $Cu_{0.25}Mo_5As_4$ (35). On the other hand, new ternary compounds of Ti_5Te_4-type were obtained by substituting molybdenum in Mo_5As_4 by a 3d element such as V, Cr, Mn, or Fe (35). Our first structural results on single crystals seem to conclude that this substitution concerns both the Mo_I and Mo_{II} positions; the unit cell parameters of the resulting compounds, e.g., $Fe_2Mo_3As_4$ and $Cr_2Mo_3As_4$, are quite similar, i.e., $a = 9.502$ Å and $c = 3.272$ Å, instead of $a = 9.600$ Å and $c = 3.278$ Å for Mo_5As_4 and are in good agreement with the normal decrease in the metallic radii of Fe and Cr compared to that of Mo ($r_{Mo} = 1.37$ Å $> r_{Cr} = 1.25$ Å $> r_{Fe} = 1.24$ Å) (16). This indicates that the substitution mechanism in binary Ti_5Te_4-type phases is possible and that mixed octahedral clusters such as $(M, Mo)_6$ can be obtained. Attempts to check this assumption for the $W_5As_{2.5}P_{1.5}$ compound are actually in progress.

A particularly striking form of the Ti_5Te_4 type is also found in the structure of $Cu_4Nb_5Si_4$ where four extra Cu atoms per formula unit occupy the metalloid voids formed by the Si atoms, between the Nb_6 chains (Fig. 4a) (36). The occurrence of relatively strong Cu–Cu bonds generate tetrahedral Cu_4 clusters with Cu–Cu intracluster distances of 2.613 Å ($\times 4$) and 2.678 Å. These clusters share common edges to form infinite linear chains along the [001] direction (Fig. 4b). The chains are isolated from each other since the smallest intercluster Cu–Cu distance is more than 3.50 Å (Fig. 4b). The insertion of these Cu_4 cluster chains induces a slight compression of the Nb_6 octahedra along the c-axis. Thus, the structure of $Cu_4Nb_5Si_4$ can be viewed as being built of infinite linear chains of Nb_6 octahedra and Cu_4 tetrahedra in a silicon network, these octahedra and tetrahedra being displayed in such a way that each copper atom in the Cu_4 cluster is linked to two Nb_6 octahedra by means of Cu–Nb bonding.

It should be noted that the compounds $Ni_4Nb_5P_4$ and $Ni_4Ta_5P_4$ have been reported to be isostructural with $Cu_4Nb_5Si_4$ (37). In that case, tetrahedral Ni_4 clusters coexist with octahedral Nb_6 or Ta_6 clusters. These examples show that the stabilization of the binaries "Nb_5Si_4," "Nb_5P_4," and "Ta_5P_4" is obtained by adding Cu_4 or Ni_4 entities in the

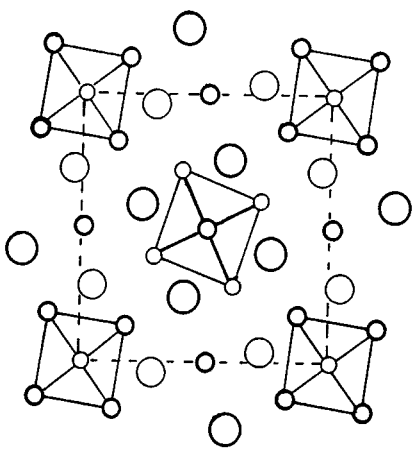

FIG. 3. Projection on the (001) plane of the structure of V_3As_2. Large circles, arsenic; small circles, vanadium; for fine and heavy circles, see legend to Fig. 2.

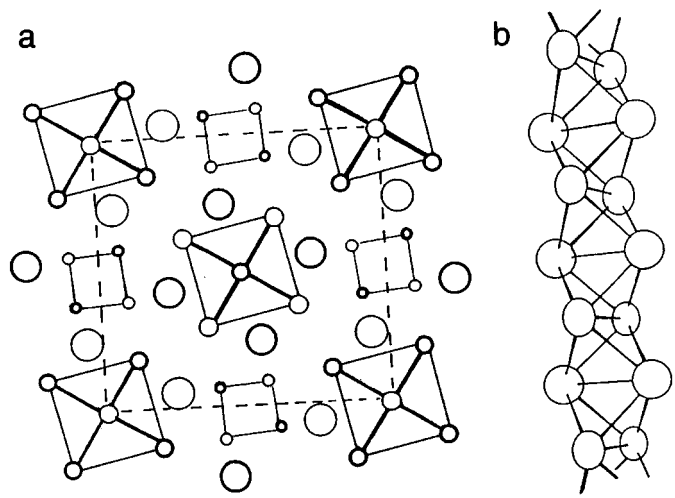

FIG. 4. Crystal structure of $Nb_5Cu_4Si_4$. (a) Projection on the (001) plane. Large circles, silicon; medium circles, niobium; small circles, copper; for fine and heavy circles, see legend to Fig. 2. Octahedral Nb_6 and tetrahedral Cu_4 clusters are emphasized. (b) Chain-like arrangement of the tetrahedral Cu_4 clusters along the c-axis.

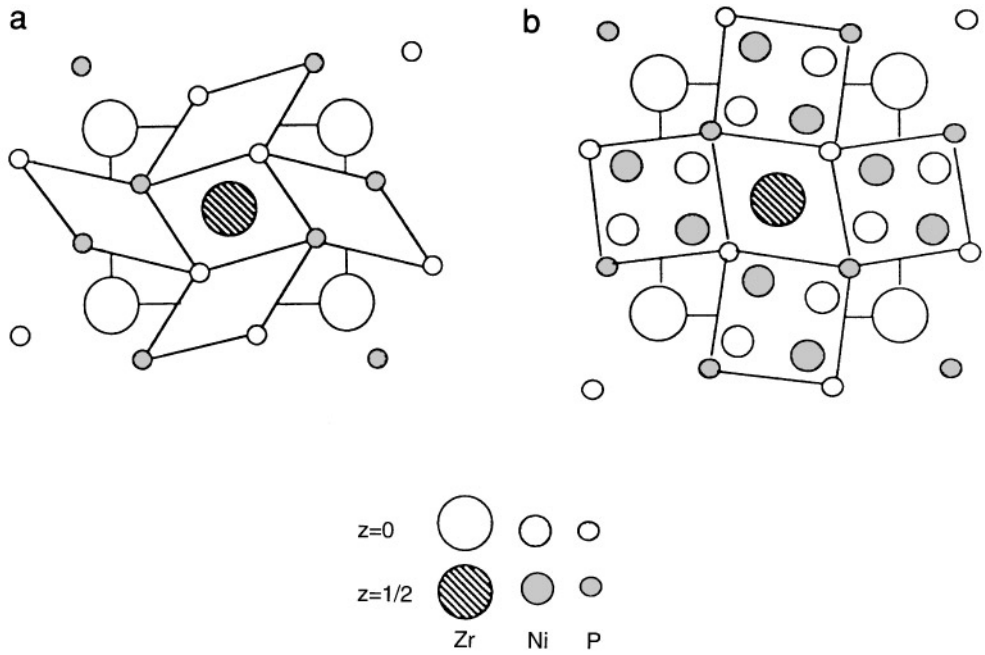

FIG. 5. Idealized structures in projection on the (001) plane of their respective unit cell. (a) Hypothetical "ZrP_2" of marcasite-type structure. (b) $ZrNi_4P_2$.

network. This suggests that the VEC of the transition metal atoms is probably too small in such "binaries" (1.8 to 2.6 per metal atom instead of 3.6 for Mo_5As_4 or $W_5As_{2.5}P_{1.5}$); the contribution of Cu or Ni atoms as electron donors seem to be absolutely required. In the case of Nb_5Sb_4 and Ta_5Sb_4 (VEC: 1.8), the occurrence of Sb–Sb bondings, owing to the larger covalent radius of Sb ($r_{Sb} = 1.41$ Å) (15), is suggested and probably induces a lower electron transfer from Nb or Ta to antimony.

Such a stabilization of a "binary" transition metal phosphide by insertion of tetrahedral Ni_4 units has also been previously observed. Thus, the structure of the ternary $ZrNi_4P_2$ compound may be considered as a marcasite-type structure with a formula unit ZrP_2 in which Ni_4 clusters are inserted (Fig. 5) (38). However, the occurrence of Ni_4 clusters in octahedral phosphorus voids of the marcasite network induces first a modification in symmetry, i.e., tetragonal ($ZrNi_4P_2$) instead of orthorhombic (marcasite), and secondly more regular metalloid sites leading to the disappearance of P–P bonds as pairs, which are characteristic of the marcasite type. Tight-binding band structure calculations on $ZrNi_4P_2$ confirmed the electron transfer of Ni_4 clusters toward Zr atoms (39). Similar calculations are in progress on the $Ni_4Nb_5P_4$ compound.

In conclusion, it is worth noting that the stabilization of transition metal phosphides by Ni_4 clusters, i.e., $Ni_4Nb_5P_4$ and $ZrNi_4P_2$, seems to occur only when the early transition metals belong to the 4*d* and 5*d* rows (Zr, Nb, Hf, Ta).

Finally, owing to the occurrence of tungsten as impurity, no physical measurements could be realized on the $W_5As_{2.5}P_{1.5}$ ternary compound but they were made on the isostructural Mo_5As_4 compound. A single crystal of this binary (dimensions, $0.10 \times 0.14 \times 0.39$ mm^3) was suitable for measurements of transport properties using a four-probe technique with silver paint contacts. The $\rho = f(T)$ curve exhibits typical metallic behavior for this compound with ρ equal to 2.8 and 36.7 μΩ cm at 4 and 300 K, respectively. Magnetic susceptibility was measured on a powder sample using a SQUID magnetometer at a field value of 1 kGauss in the temperature range 80 to 300 K. A nearly temperature independent paramagnetism ($\chi = 47 \times 10^{-6}$ cm^3/mol at room temperature) was found which confirmed the metallic behavior of the Mo_5As_4 compound. By extension, a similar conclusion can be made for the new isostructural ternary compound $W_5As_{2.5}P_{1.5}$, which is in good agreement with the presence of itinerant electrons involving numerous metal–metal bondings.

REFERENCES

1. J. B. Taylor, L. D. Calvert, and M. R. Hunt, *Can. J. Chem.* **43,** 3045 (1965).
2. P. Jensen, A. Kjekshus, and T. Skansen, *Acta Chem. Scand.* **20,** 403 (1966).
3. S. Furuseth and A. Kjekshus, *Acta Crystallogr.* **18,** 320 (1965).
4. P. Jensen, A. Kjekshus, and T. Skansen, *Acta Chem. Scand.* **20,** 1003 (1966).

5. P. Jensen and A. Kjekshus, *Acta Chem. Scand.* **20,** 1309 (1966).
6. R. Guérin, M. Sergent, and J. Prigent, *Mater. Res. Bull.* **10,** 957 (1975).
7. R. Guérin, Thèse d'Etat, Rennes, France, 1976.
8. R. Guérin, M. Sergent, and J. Prigent, *C. R. Acad. Sci.* **274,** 1278 (1972).
9. D. Louër, *Mater. Sci. For.* **79–82,** 17 (1991).
10. D. Louër and J. I. Langford, *J. Appl. Crystallogr.* **21,** 430 (1988).
11. D. A. Boultif and D. Louër, *J. Appl. Crystallogr.* **21,** 987 (1991).
12. A. D. Mighell, C. R. Hubbard, and J. K. Stalick, "NBS*AIDS80: A Fortran Program for Crystallographic Data Evaluation," Nat. Bur. Stand. Techn. Note 1141, 1981. [NBS*AIDS83 is an expanded version of NBS*AIDS80].
13. International Centre for Diffraction Data, Newtown Square, PA, USA.
14. International Centre for Diffraction Data, "NIST CDF database," Newtown Square, PA, USA.
15. L. Pauling, "Nature of the Chemical Bond," 3rd ed. Cornell Univ. Press, Ithaca, New York, 1960.
16. F. Laves, "Theory of Alloy Phases." Am. Soc. Metals, Cleveland, Ohio, 1956.
17. J. Rodriguez-Carvajal, "FULLPROF: A Program for Rietveld Refinement and Pattern Matching Analysis," Collected Abstracts of Powder Diffraction Meeting, Toulouse, France, p. 127, 1990.
18. R. A. Young and D. B. Wiles, *J. Appl. Crystallogr.* **14,** 149 (1981).
19. P. Bénard, D. Louër, N. Dacheux, V. Brandel, and M. Genet, *Chem. Mater.* **6,** 1049 (1994).
20. S. Ihmaïne, C. Perrin, and M. Sergent, *Croatica Chem. Acta* **68,** 877 (1995).
21. S. Ihmaïne, C. Perrin, and M. Sergent, submitted for publication.
22. T. C. Zietlow, W. P. Schaefer, B. Sadeghi, N. Hua, and H. B. Gray, *Inorg. Chem.* **25,** 2195 (1986).
23. T. Saito, A. Yoshikawa, T. Yamagata, H. Imoto, and K. Unoura, *Inorg. Chem.* **28,** 3588 (1989).
24. X. Zhang and R. E. McCarley, *Inorg. Chem.* **34,** 2678 (1995).
25. G. M. Ehrlich, C. J. Warren, D. A. Vennos, D. M. Ho, R. C. Haushalter, and F. J. DiSalvo, *Inorg. Chem.* **34,** 4454 (1995).
26. D. Eberle and K. Schubert, *Z. Metallkd.* **59,** 306 (1968).
27. F. Gronvold, H. Haraldsen, P. Pedersen, and T. Tufte, *Rev. Chim. Minér.* **6,** 215 (1969).
28. E. Röst and L. Gjertsen, *Z. Anorg. Allg. Chem.* **328,** 300 (1964).
29. S. Furuseth and A. Kjekshus, *Acta Chem. Scand.* **18,** 1180 (1964).
30. K. Selte and A. Kjekshus, *Acta Chem. Scand.* **17,** 2560 (1963).
31. S. Furuseth and A. Kjekshus, *Acta Chem. Scand.* **19,** 95 (1965).
32. A. Simon, *Angew. Chem. Int. Ed. Engl.* **20,** 1 (1981).
33. R. Berger, *Acta Chem. Scand. A* **31,** 287 (1977).
34. K. S. Nanjundaswamy and J. Gopalakrishnan, *J. Chem. Soc. Dalton Trans.* **1,** 1 (1988).
35. S. Députier and R. Guérin, *J. Alloys Comp.*, in press.
36. E. Ganglberger, *Monatsh. Chem.* **99,** 546 (1968).
37. R. Berger, P. Phavanantha, and M. Mongkolsuk, *Acta Chem. Scand. A* **34,** 77 (1980).
38. J. Y. Pivan, R. Guérin, E. H. El Ghadraoui, and M. Rafiq, *J. Less-Common Met.* **153,** 285 (1989).
39. A. Le Beuze, M. C. Zerrouki, R. Lissilour, R. Guérin, and W. Jeitschko, *J. Alloys Comp.* **191,** 53 (1993).